Lithium and Deuterium NMR Studies of Acid-Leached Layered Lithium Manganese Oxides

Younkee Paik,[†] Clare P. Grey,*[,†] Christopher S. Johnson,[‡] Jeom-Soo Kim,[‡] and Michael M. Thackeray[‡]

Department of Chemistry, State University of New York, Stony Brook, New York 11794-3400, and Chemical Technology Division, Argonne National Laboratory, Argonne, Illinois 60439

Received June 24, 2002. Revised Manuscript Received October 1, 2002

^{6}Li and ^{2}H MAS NMR in conjunction with X-ray diffraction is used to study the acid leaching of the layered Mn(IV) compound Li_2MnO_3 (i.e., $Li[Li_{0.33}Mn_{0.67}]O_2$). Lithium NMR shows that the lithium ions are progressively removed from the lithium layers during leaching, the reduction in lithium content in the layers correlating directly with the concentration of a new local environment for lithium that contains both manganese ions and protons in the first cation coordination sphere. The composition of these samples may be written as $H_{1-x}Li_x[Li_{0.33}Mn_{0.67}]O_2$, indicating that H^+/Li^+ ion exchange has occurred. ^{2}H MAS NMR shows unequivocally that deuterons are present in these structures, following leaching in D_2SO_4/D_2O. X-ray diffraction confirms that leaching is associated with the shearing of the oxygen layers to form a structure with an AABBCC stacking sequence of the oxygen layers. This stacking sequence is also found in isostructural compound $HCrO_2$. The hydrogen bonding between the oxygen layers is proposed to provide the driving force for oxygen shearing so as to minimize the O−O distances between the "AA", "BB", and "CC" layers to generate stronger hydrogen bonding. Li^+/H^+ ion exchange is also accompanied by the loss of Li_2O from the structure, which is more pronounced for Li_2MnO_3 samples calcined for shorter times. These samples can be cycled as positive electrodes (versus Li), providing capacities of more than 150 mA h g^{-1}.

1. Introduction

Acid leaching of lithium manganates represents one possible strategy for synthesizing new or modified manganese oxide electrodes for lithium batteries. In an early report, Hunter showed that the delithiated spinel λ-MnO_2 could be produced by acid treatment of $LiMn_2O_4$.[1] Using a similar approach, new layered manganese oxides were produced by acid treatment of the Mn(IV) oxide Li_2MnO_3.[2] These materials show high electrode capacities (150−180 mA·h/g) when cycled between 3.8 and 2.0 V in rechargeable lithium cells[3] and convert more slowly to a spinel-type phase compared to layered $LiMnO_2$ electrodes. Li_2MnO_3 has an ordered rock-salt structure with a layered configuration that can be represented in conventional notation (for the ABO_2 layered materials) as $Li[Li_{0.33}Mn_{0.67}]O_2$ with alternating Li and $[LiMn_2]$ cation layers (Figure 1). It was proposed that delithiation of Li_2MnO_3 occurs by the reaction

$$Li_2MnO_3 + 2\delta H^+ \rightarrow Li_{2-2\delta}MnO_{3-\delta} + \delta H_2O + 2\delta Li^+ \quad (1)$$

with the possibility of some H^+ ion exchange for Li^+ in the structure.[2] The acid-leaching process was shown to be accompanied by a shearing of the oxygen close-packed layers to form a layered structure in which the manganese ions and some lithium ions remain in octahedral sites in one layer, the residual lithium ions occupying a trigonal prismatic coordination site in alternate layers.[4] More recently, Li_2MnO_3 with much smaller particle sizes was synthesized, resulting in more complete acid leaching.[3] Ooi and co-workers have investigated the acid leaching of a single crystal of Li_2MnO_3 under hydrothermal conditions. Their work on this and related systems was, in part, motivated by their ongoing studies of the ion-exchange properties of manganese oxides and hydroxides.[5,6] They suggested that the lithium ions between the transition-metal

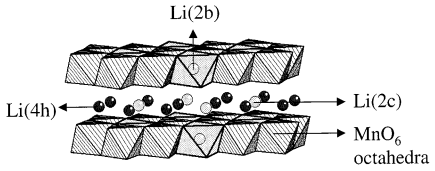

Figure 1. Structure of Li_2MnO_3 showing the Li and $[Li_{0.33}Mn_{0.67}]$ layers.

* To whom correspondence should be addressed. Fax: 631-632-5731. E-mail: cgrey@sbchem.sunysb.edu.
[†] State University of New York.
[‡] Argonne National Laboratory.

(1) Hunter, J. C. *J. Solid State Chem.* **1981**, *39*, 142.
(2) Rossouw, M. H.; Thackeray, M. M. *Mater. Res. Bull.* **1991**, *26*, 463.
(3) Johnson, C. S.; Korte, S. D.; Vaughey, J. T.; Thackeray, M. M.; Bofinger, T. E.; Shao-Horn, Y.; Hackney, S. A. *J. Power Sources* **1999**, *81−82*, 491.
(4) Rossouw, M. H.; Liles, D. C.; Thackeray, M. M. *J. Solid State Chem.* **1993**, *104*, 464.
(5) Feng, Q.; Kanoh, H.; Miyai, Y.; Ooi, K. *Chem. Mater.* **1995**, *7*, 1722.
(6) Tang, W.; Kanoh, H.; Yang, X.; Ooi, K. *Chem. Mater.* **2000**, *12*, 3271−3279.

10.1021/cm0206385 CCC: $22.00
Published on Web 11/12/2002

layers are removed by two stepwise mechanisms: first, by ion-exchange reaction with the protons to form $Li_{1-x}H_x[Li_{0.33}Mn_{0.67}]O_2$ and, second, by lithium dissolution as lithia (Li_2O). The latter was accompanied by the growth of α-MnO_2 on the surface of the single crystals before conversion to a γ-MnO_2 phase.[6]

Locating and quantifying the number and types of protons (hydroxyl vs structural water) in these samples is key to elucidating the acid-leaching mechanisms in these systems. These protons may also play an important role in controlling how these compounds function as electrode materials. For example, in electrolytic manganese oxide (EMD), the nature and concentration of the protons affects the performance of EMD electrodes when used in both alkaline and lithium primary cells.[7] Similar phenomena can be found in the electrochemistry of vanadium and iron phosphates,[8] which can contain structural water. In addition, these Li^+/H^+ ion-exchange reactions are significant in understanding the electrochemical behavior of Li_2MnO_3 electrodes that has been reported by Kalyani et al.[9] and by Robertson and Bruce.[10]

In this work, we use a combination of ^{6}Li and ^{2}H MAS NMR spectroscopy, techniques that have been shown to be useful in studying related paramagnetic manganese materials,[11,12] to investigate the leaching process of Li_2MnO_3. We show that we can detect the presence of deuterons formed following acid treatment in deuterated solvents and propose an explanation for the shearing of the manganese layers, which occurs during the acid leaching. A preliminary report of this work has been published in ref 13.

2. Experimental Section

Li_2MnO_3 precursor materials were prepared in air by solid-state reactions. Stoichiometric amounts of LiOH and γ-MnO_2 were used as the lithium and manganese sources. They were well ground together and fired by using two different heating procedures. Li_2MnO_3 (sample A) was prepared by heating first at 465 °C for 24 h and then at 500 °C for 48 h. Li_2MnO_3 (sample B) was prepared by heating at 650 °C for 36 h. The Li_2MnO_3 precursors were acid-leached at ambient temperatures in 2.5 M H_2SO_4 (or D_2SO_4). The Li_2MnO_3/acid slurries were stirred for between 1 and 120 h, filtered, and then washed. The samples are labeled Li_2MnO_3(A or B)_*n*, where *n* indicates the number of hours of acid leaching. Powder X-ray diffraction data of these samples were collected on an automated Siemens D-5000 powder diffractometer with Cu Kα radiation.

^{6}Li and ^{2}H MAS NMR experiments were performed at 29.45 and 30.72 MHz, respectively, with a CMX-200 spectrometer. A Chemagnetics probe equipped with 4-mm rotors for MAS was used for the ^{2}H and some ^{6}Li MAS NMR experiments; a MAS probe, built by Samoson and co-workers,[14] equipped with 2-mm rotors for very high sample spinning (≈45 kHz), was used for fast-MAS ^{6}Li NMR. Spectra were recorded with a rotor synchronized Hahn-echo pulse sequence, with an evolution period of one rotor period.

Electrochemical cycling experiments were carried out with 2032 coin cell hardware (Hohsen). Electrodes consisted of the active oxide (86 wt %), acetylene black (3.5 wt %), graphite (3.5 wt %), and polymer binder (poly(vinylidene difluoride), 7 wt %). The electrodes were dried at 90 °C for 24 h under vacuum, before the cells were constructed in a helium-filled glovebox. 1 M $LiPF_6$ in 1:1 DEC:EC (diethyl carbonate:ethylene carbonate) was used as the electrolyte. Cells were cycled using a Maccor Series 2000 control unit in galvanostatic mode.

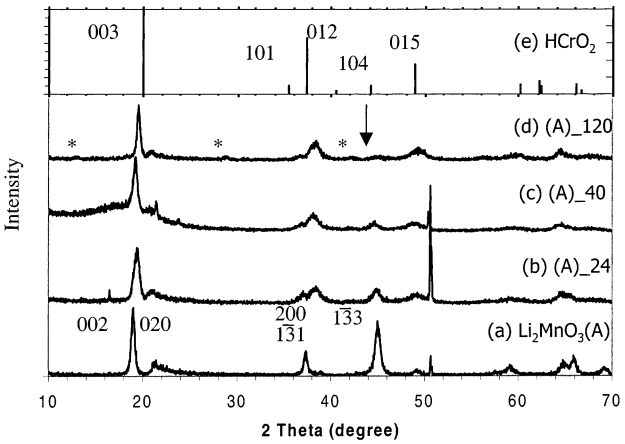

Figure 2. X-ray powder diffraction patterns of (a) the precursor Li_2MnO_3(A) and (b)−(d) its acid-leached derivatives (the leaching time in hours, *n*, are marked as (A)_*n*). (e) Joint Committee on Powder Diffraction Standards (JCPDS) file for $HCrO_2$ (#700621). The Li_2MnO_3 and $HCrO_2$ reflections are indexed with the *C*2/*c* and $R\bar{3}m$ space groups, respectively. The Li_2MnO_3 $1\bar{3}3$ reflection, marked by an arrow, decreases in intensity upon acid leaching (see text). Weak reflections from an α-MnO_2 impurity in Li_2MnO_3(A)_120 sample are indicated with asterisks. The broad hump centered around 18° (2θ) in the pattern of Li_2MnO_3(A)_40 is due to the grease on the sample holder. The sharper reflections at approximately 21.5° and 50.7° (2θ), seen in the patterns of Li_2MnO_3(A) and Li_2MnO_3(A)_24 and _40, are due to the sample holder itself.

3. Results

3.1. Acid-Leaching Mechanism. *3.1.1. Characterization of the Structural Changes by X-ray Diffraction.* The X-ray diffraction (XRD) powder patterns of the precursor Li_2MnO_3(A) and its acid-leached derivatives are shown in Figure 2. The reflections for Li_2MnO_3(A) are broad, reflecting the small particle sizes of this material. A gradual decrease in the intensity of the reflections from the Li_2MnO_3 phase is observed with increased acid-leaching time, the change being most readily followed by monitoring the decrease in the intensity of the Li_2MnO_3 $\{1\bar{3}3\}$ set of reflections at approximately 45° 2θ. This is accompanied by the growth of a new phase, with a characteristic reflection at approximately 38.5° 2θ. The new phase is consistent with that seen in an earlier study, in which it was shown that the acid-leaching process is accompanied by a shear of the close-packed oxygen planes to trigonal prismatic stacking.[4] The {002} reflection of Li_2MnO_3 shifts slightly to a higher 2θ value, consistent with a decrease in the *c* parameter on acid leaching. In contrast, the Li_2MnO_3 {020} reflection, which is indicative of Li:Mn ordering in the *ab*-plane, is unchanged, suggesting that the ordering of the manganese ions in the transition-metal

(7) Ruetschi, P.; Giovanoli, R. *J. Electrochem. Soc.* **1988**, *135*, 2663.
(8) Dupre, N.; Gaubicher, J.; Mercier, T. L.; Wallez, G.; Angenault, J.; Quarton, M. *Solid State Ionics* **2001**, *140*, 209.
(9) Kalyani, P.; Chitra, S.; Mohan, T.; Gopukumar, S. *J. Power Sources* **1999**, *80*, 103.
(10) Robertson, A. D.; Bruce, P. G. *Extended Abstr. 85*, 11th International Meeting on Lithium Batteries, Monterey, June 23−28, 2002.
(11) Lee, Y. J.; Wang, F.; Grey, C. P. *J. Am. Chem. Soc.* **1998**, *120*, 12601.
(12) Paik, Y.; Osegovic, J. P.; Wang, F.; Bowden, W.; Grey, C. P. *J. Am. Chem. Soc.* **2001**, *123*, 9367.
(13) Paik, Y.; Grey, C. P.; Johnson, C. S.; Kim, J.-S.; Thackeray, M. M. *Extended Abstr. 290*, 11th International Meeting on Lithium Batteries, Monterey, June 23−28, 2002.
(14) Du, L. S.; Samoson, A.; Tuherm, T.; Grey, C. P. *Chem. Mater.* **2000**, *12*, 3611.

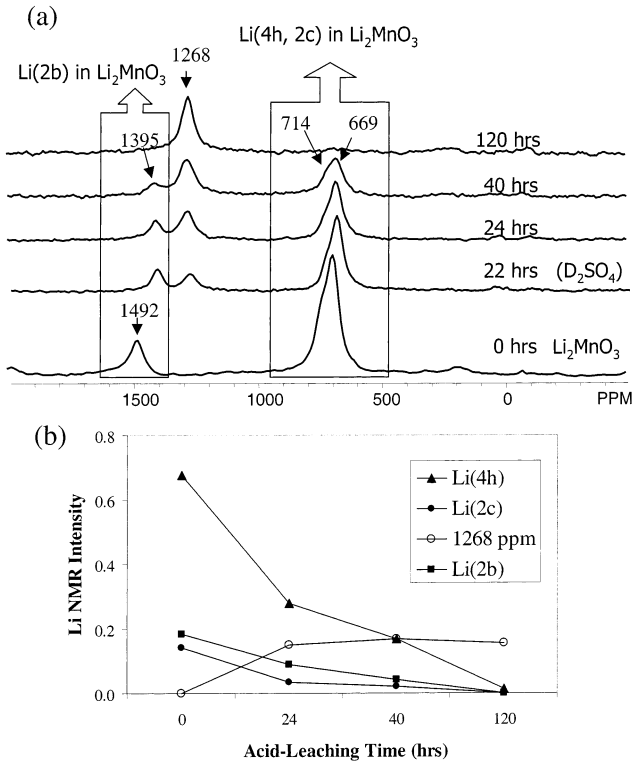

Figure 3. (a) ^{6}Li MAS NMR spectra of Li_2MnO_3(A) and its acid-leached derivatives. Leaching time is marked on each spectrum. MAS speeds of 36−40 kHz were used. (b) The plot of Li NMR intensity vs acid-leaching time. The sum of the peak intensities from Li_2MnO_3 is normalized to unity.

layers is preserved in the acid-leached material. Note that XRD cannot be readily used to determine whether this Mn ordering is associated with Li ordering or vacancy ordering (caused by Li removal) in the Mn layers, due to the weak scattering power of lithium. These two possibilities can be distinguished by the Li NMR experiments described in the next section.

3.1.2. Probing the Changes in Lithium and Deuterium Local Environments with NMR Spectroscopy. ^{6}Li MAS NMR spectra were acquired to understand the change in lithium local environments upon acid leaching (Figure 3). Three isotropic resonances are observed from the precursor Li_2MnO_3(A) at 736, 777, and 1492 ppm, which can be assigned to lithium ions in 4h, 2c, and 2b sites (see Figure 1), respectively, based on the relative intensities of these resonances and their Fermi-contact shifts.[15−17] A gradual decrease in intensity of the resonance due to lithium between the transition-metal layers, that is, lithium in the 4h (669 ppm) and 2c (714 ppm) sites, is seen, as a function of leaching time. Thus, these ^{6}Li NMR spectra may be used to estimate the amount of lithium extracted from the lithium layers (Figure 3b). The shift in the 2b resonance of Li_2MnO_3 from 1492 ppm in (a) to 1395 ppm in (b)−(d) is due to slightly different experimental conditions used to acquire these spectra. (The spectra in (a) were acquired while blowing room temperature air over the MAS rotor; thus, the sample was maintained at a slightly lower

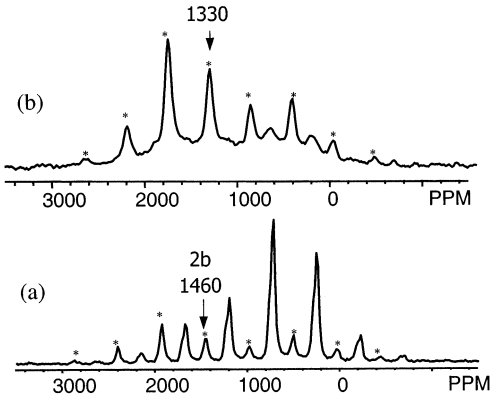

Figure 4. ^{6}Li MAS NMR spectra showing the isotropic resonance and sideband pattern (*) of the Li 2b resonance of Li_2MnO_3(A): (a) before and (b) after 120 h of acid-leaching treatment. MAS speeds of 13−14 kHz were used.

temperature in (a) than in (b)−(d), accounting for the larger shift.) The decrease in the Li 2b resonance (1492−1395 ppm) is accompanied by the growth of a new resonance at 1268 ppm. The increase in the intensity of this new resonance is exactly the same, within the experimental error, as the decrease in the intensity of the Li 2b resonance. Furthermore, both these resonances show very similar sideband envelopes (Figure 4). The sidebands in the ^{6}Li spectra of lithium manganates primarily arise from the dipolar coupling between ^{6}Li and the unpaired electrons on the manganese ions and are extremely sensitive to the spatial arrangements of the manganese ions around the lithium spins. Specifically, the asymmetry of the 2b Li_2MnO_3 resonance is characteristic of lithium symmetrically surrounded by manganese ions in a planar arrangement.[15] Thus, the new resonance must also arise from a coordination environment that is similar to that of the 2b sites in Li_2MnO_3.

A weaker resonance at 700 ppm, due to lithium in the lithium layers in residual Li_2MnO_3-like particles, is observed more clearly in the slower spinning ^{6}Li NMR spectrum (Figure 4). Nonetheless, the lithium content in the lithium layers still corresponds to <2% of its initial value. The apparent enhancement of the intensity of this resonance at low spinning speeds is a consequence of the smaller spinning sideband manifold of the 700 ppm, in comparison to the 1400 or 1300 ppm resonances; this smaller sideband intensity will result in an enhancement of the 700 ppm isotropic resonance, relative to the 1400/1300 ppm isotropic resonances at slow spinning speeds. The reduction in sideband intensity of this resonance is ascribed to the smaller number of manganese ions in the first cation coordination sphere of the lithium in the Li layers.

The ^{2}H MAS NMR spectra of Li_2MnO_3(A), leached at 25 °C in D_2SO_4 for 22 h, is shown in Figure 5. The spectrum is dominated by one isotropic resonance at 390 ppm, with a large sideband manifold. The ^{2}H NMR line shapes of paramagnetic materials have been studied by a number of authors.[18,19] In our previous work, ^{2}H MAS NMR (hyperfine) shifts of 300−425 ppm at ambient

(15) Lee, Y. J.; Grey, C. P. *J. Phys. Chem. B* **2002**, *106*, 3576.
(16) Morgan, K. R.; Collier, S.; Burns, G.; Ooi, K. *J. Chem. Soc., Chem. Commun.* **1994**, 1719.
(17) Mustarelli, P.; Massarotti, V.; Bini, M.; Capsoni, D. *Phys. Rev. B* **1997**, *55*, 12018.
(18) Lin, T.; DiNatale, J. A.; Vold, R. R. *J. Am. Chem. Soc.* **1994**, *116*, 2133.
(19) Siminovitch, D. J.; Rance, M.; Jeffrey, K. R. *J. Magn. Reson.* **1984**, *58*, 62.

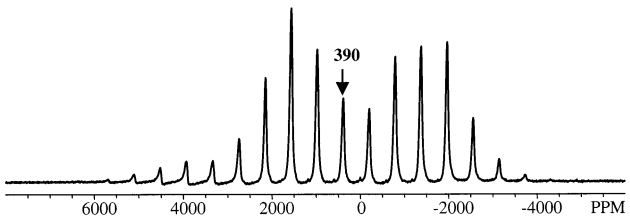

Figure 5. ^{2}H MAS NMR spectrum of acid-leached Li_2MnO_3-(A). Acid treatment was carried out in 2.5 M D_2SO_4 at 25 °C for 22 h. MAS speed was ≈18 kHz.

temperature were observed from deuterated manganese(III) hydroxides such as manganite and groutite.[12] We showed that the arrangements of the first cation coordination sphere of manganese ions around the hydroxyl group, and the coordination geometry of the oxygen atom (i.e., sp^2 or sp^3), determined the size and direction of the ^{2}H NMR shift of these Mn(III) compounds. Similarly, the large ^{2}H NMR shift (≈390 ppm) in these acid-leached systems can be ascribed to a through-bond hyperfine interaction between the deuterons and adjacent manganese ions, via the intervening oxygen atoms. The shape of the spinning sideband manifold resembles, to a first approximation, a Pake Doublet. The Pake Doublet line shape is caused by the nuclear quadrupole interaction and is consistent with a rigid $I = 1$ spin in a close to axially symmetric local environment. This indicates that the deuterons are rigidly bound to the oxygen sites (i.e., the protons are rigid on a time scale governed by the ^{2}H MAS NMR experiment (≈0.1 ms).[20] Furthermore, these line shapes are *not* consistent with those of bound isolated water molecules, which typically show distinctive line shapes as a result of the so-called 180° flips of the water molecules that generally occur at ambient temperatures.[21] The deviation of the ^{2}H line shape from that of an ideal, symmetric Pake Doublet is due to the dipolar interaction between the deuterons and unpaired electrons located on the manganese ions. These observations are all consistent with the first ion-exchange mechanism proposed by Ooi and co-workers.[6] Only one deuteron environment is observed, which suggests that the deuterons bind to intact $[Li_{0.33}Mn_{0.67}]$ layers and that substantial concentrations of different local environments for deuterium have *not* been created, due to, for example, Li^+ or Mn^{4+} vacancies.

The clear observation of protons/deuterons in these samples allows us to account for the ^{6}Li NMR shift of a new Li environment. The ^{6}Li resonance at approximately 1300 ppm can be assigned to the local environment $Li(O(H/D)Mn)_6$, the "(H/D)" indicating that the nearby oxygen atoms are coordinated/hydrogen-bonded to H/D. The shift of ≈100 ppm of this resonance from the shift of the $Li(OMn)_6$ environment (the 2b site) in Li_2MnO_3 is consistent with covalent H−O binding to the intervening oxygen atoms, which might be expected to reduce the Li−O−Mn orbital overlap and thus the hyperfine shift. The ^{2}H results, in conjunction with the ^{6}Li data, indicate that the formula of Li_2MnO_3(A)_120 can be written as $H[Li_{0.33}Mn_{0.67}]O_2$, ignoring the small residual concentration of Li_2MnO_3 (<1.4 wt %). Consistent with the H-analysis from NMR, a thermogravimetric analysis of the same sample indicated that the material loses 17.2% of its initial weight, following heat treatment at 220 °C under an argon atmosphere. X-ray diffraction of the heat-treated sample (not shown) showed that a spinel phase was formed, allowing the following reaction to be written for the decomposition reaction:

$$H[Li_{0.33}Mn_{0.67}]O_2 \rightarrow {}^1/_3LiMn_2O_4 + {}^1/_2H_2O + {}^1/_4O_2(g) \quad (2)$$

A theoretical weight loss of 23% is predicted for this reaction, which is reasonably close to the experimental result. The ^{6}Li NMR spectrum of a partially leached material, acquired at 250 °C, resembles that of a lithium-rich spinel $Li_{1+x}Mn_{2-x}O_4$, consistent with the presence of residual lithium ions in the lithium layers.

3.1.3. Investigation of the Differences in Acid-Leaching Reactivity and Li_2MnO_3 Synthesis Conditions. The ^{2}H and ^{6}Li MAS NMR spectra of the acid-leached Li_2MnO_3-(B) sample, leached in 2.5 M D_2SO_4 (in D_2O) for 6 h, are similar to the spectrum of Li_2MnO_3(A)_120 (Figure 3a) and the ^{2}H MAS NMR spectrum shown in Figure 5. The ^{6}Li NMR spectra shows only one isotropic resonance at 1330 ppm that can be assigned to lithium in transition-metal layers, all of the lithium ions in the lithium layer having been extracted and/or ion-exchanged with deuterons. Thus, this Li_2MnO_3(B) phase, which was prepared at a higher temperature but with shorter heating time (650 °C, 36 h) than the Li_2MnO_3(A) phase (465 °C/500 °C, 72 h), shows much higher acid-leaching reactivity. This suggests that the rates of acid delithiation and/or ion exchange of the parent Li_2MnO_3 materials are sensitive to their method of preparation and resulting particle size. These data are consistent with our earlier studies of Li_2MnO_3 leaching, where complete reaction was achieved for materials synthesized at low temperature (400−500 °C), while incomplete leaching was seen for samples prepared at 700 °C.[2−4]

A decrease in *both* the lithium and deuterium NMR intensities was observed for more prolonged acid leaching of the Li_2MnO_3(B) sample (24 h; 2.5 M D_2SO_4 (in D_2O)). This is consistent with previous studies,[6] indicating that the dissolution of lithium as lithia (Li_2O) occurs in conjunction with the ion-exchange mechanism. The ^{6}Li MAS NMR spectrum of Li_2MnO_3(B)_24 (Figure 6a) contains a single resonance due to lithium in the Li/Mn layers of the leached material. The ^{2}H NMR spectrum of this material (Figure 6b) is very similar to the spectra of Li_2MnO_3(B)_6 and contains a single isotropic resonance at 389 ppm. This provides clear evidence that the deuterium local environments have not changed following more extended leaching. The ^{2}H NMR sideband pattern and isotropic shift are also similar to that of Li_2MnO_3(A)_22 (Figure 5), even though Li_2MnO_3(A)_22 contains some residual lithium ions in the Li_2MnO_3 lithium layers. The compositions of these samples were determined by careful spin counting of the ^{2}H and ^{6}Li intensities, using deuterated manganite (MnOOD) and Li_2MnO_3, as ^{2}H and ^{6}Li standards, respectively. The lithium content in the $[Li_{0.33}Mn_{0.67}]$ layers was found to decrease from 5.9 wt % in the precursor material Li_2MnO_3(B) to 3.6 and 2.3 wt % for

(20) Maricq, M. M.; Waugh, J. S. *J. Chem. Phys.* **1979**, *70*, 3300.
(21) Ackerman, J. L.; Eckman, R.; Pines, A. *Chem. Phys.* **1979**, *42*, 423.

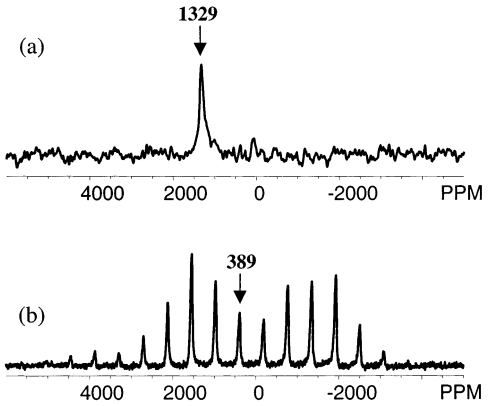

Figure 6. (a) ^{6}Li and (b) ^{2}H MAS NMR spectra of Li_2MnO_3 (B)_24, acid-leached at 25 °C in 2.5 M D_2SO_4 (in D_2O) for 24 h. Isotropic resonances are marked on each spectrum. The MAS speeds were 40 kHz for the ^{6}Li and 18 kHz for the ^{2}H MAS spectra.

Table 1. Chemical Composition of the Acid-Leached Samples, Calculated from the NMR Data[a]

sample	composition
Li_2MnO_3(A)	$Li[Li_{0.33}Mn_{0.67}]O_2$
Li_2MnO_3(A)_24	$Li_{0.33}H_{0.67}[Li_{0.33}Mn_{0.67}]O_2$
Li_2MnO_3(A)_40	$Li_{0.19}H_{0.81}[Li_{0.33}Mn_{0.67}]O_2$
Li_2MnO_3(A)_120	$H[Li_{0.33}Mn_{0.67}]O_2$
Li_2MnO_3(B)	$Li[Li_{0.33}Mn_{0.67}]O_2$
Li_2MnO_3(B)_6	$D_{0.57}[Li_{0.23}Mn_{0.77}]O_{1.94}$
Li_2MnO_3(B)_24	$D_{0.22}[Li_{0.17}Mn_{0.83}]O_{1.86}$

[a] The oxygen contents of the (A) series were assumed to remain unchanged on acid leaching, allowing the hydrogen contents of these samples to be estimated.

(B)_6 and (B)_24, respectively, while the deuteron content dropped from 0.65 for (B)_6 to 0.32 wt % for (B)_24. Values for the compositions of the two samples of $D_{0.57}[Li_{0.23}Mn_{0.77}]O_{(2)}$ and $D_{0.22}[Li_{0.17}Mn_{0.83}]O_{(2)}$ were estimated for Li_2MnO_3(B)_6 and Li_2MnO_3(B)_24, respectively, where the formulas were calculated by assuming that no oxygen vacancies are formed and that the formulas can be written as $A[Mn_xB_{1-x}]O_2$ (i.e., there are no cation vacancies in the Li/Mn layers). The oxygen contents are, therefore, written in parentheses, indicating that these are assumed. Some vacancies must be present to maintain charge balance, resulting in compositions such as $D_{0.22}[Li_{0.17}Mn_{0.83}]O_{1.86}$ for (B)_24. Thus, it is clear that some leaching of Li_2O has occurred in these samples (reaction (1)). These formulas should be contrasted with those for the Li_2MnO_3(A) series, which can all be expressed by the formula $H_{1-y}Li_y[Li_{0.33}Mn_{0.67}]O_2$ ($1 \geq y \geq 0$; the H content is not quantified, but is inferred based on charge balance considerations), where no evidence for Li_2O dissolution is observed, even after 120 h of leaching. The compositions of all the samples are summarized in Table 1.

Taken together, the results for the (A) and (B) series suggest that the leaching of Li_2O must also be associated with the removal of a substantial concentration of ion-exchanged, structural deuterons (or protons), via reactions such as

$$H_{1-y}Li_y[Li_{0.33}Mn_{0.67}]O_2 \rightarrow 0.67MnO_2 + (0.165 + y/2)Li_2O + (1/2 - y/2)H_2O \quad (3)$$

These results are qualitatively similar to those of Ooi and co-workers, where H^+/Li^+ exchange was seen to occur in their hydrothermal treatments of Li_2MnO_3, for $[H^+]:[Li^+]$ ratios of up to 0.15 ($[Li^+]$ and $[H^+]$ indicating the total lithium content in the starting material and total proton content in the aqueous H_2SO_4 solutions used for leaching, respectively).[6] The dissolution mechanism, which results in a reduction of *both* the H and Li content, occurred in competition with the ion-exchange mechanism (which results in a higher proton content), for increased acid concentration, both mechanisms occurring simultaneously for $[H^+]:[Li^+] \geq 0.25$. A maximum proton content was achieved in Ooi and co-workers' study for $[H^+]:[Li^+] = 0.75$, resulting in a final composition of $Li_{0.48}H_{0.74}MnO_{2.6}$.[6]

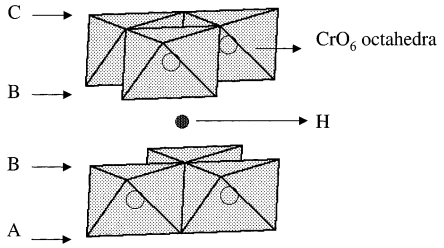

Figure 7. Oxygen stacking sequence and proton bonding environment in hydrogen chromate, from ref 22.

Structural Implications. The oxygen close-packing arrangement "ABBCCA" in the acid-leached Li_2MnO_3 compound is identical to that found in $HCrO_2$, which contains [O···H−O] hydrogen-bonding arrangements for the protons and short O−O distance (2.49 for O−H−O and 2.55 Å for O−D−O groups) between the chromium oxide layers (Figure 7).[22] $HCrO_2$ also adopts the same space group, $R\bar{3}m$, as the oxygen array of the acid-leached material;[22] its powder diffraction pattern is shown in Figure 2 for comparison with those of the leached materials. (Note that in $HCrO_2$ the Cr ions are trivalent and fully occupy the octahedral sites of one layer, thereby satisfying the requirements for $R\bar{3}m$ symmetry, whereas in the acid-leached Li_2MnO_3 samples the transition-metal layer contains both tetravalent Mn and monovalent Li ions; ordering of the Mn and Li ions in a $[Li_{0.33}Mn_{0.67}]$ arrangement lowers the crystal symmetry of these compounds below $R\bar{3}m$.) The oxygen atoms in $HCrO_2$ form a trigonal pyramid arrangement in the O−O layers, with each proton being hydrogen-bonded between two oxygen atoms in these layers. The unit cell parameters, *a* and *c*, are 2.985 and 13.48 Å for $HCrO_2$ and 2.903 and 13.803 Å for the leached materials, respectively.[4] The slightly smaller value of the *c* parameter for the chromate is consistent with the shift of the 003 reflection to larger 2θ. The *a* parameter of the manganate is smaller, which is again consistent with the presence of Li in the transition-metal layers.

The shortest O−O distances across the lithium layers of Li_2MnO_3 are 3.049 and 3.121 Å (Figure 8).[23] This O−O distance is much too long for a *strong* hydrogen bond. By shearing of the oxygen layers to form the $HCrO_2$ structure, the O−O distances are reduced significantly to 2.5 Å (a distance consistent with strong hydrogen bonding); this should represent a strong driving force for the transformation between the two structures on acid leaching.

(22) Hamilton, W.; Ibers, J. A. *Acta Crystallogr.* **1963**, *16*, 1209.
(23) Strobel, P.; Lambert-Andrau, B. *J. Solid State Chem.* **1988**, *75*, 90.

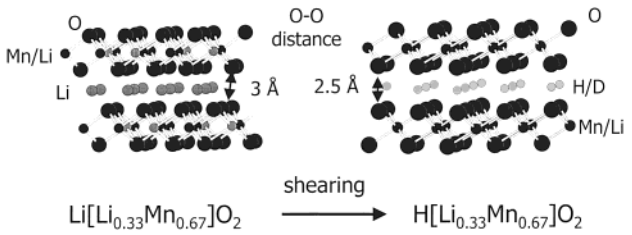

Figure 8. A schematic showing how shearing of the oxygen layers results in a reduction of the O−O separation, across the lithium layers, by ≈0.5 Å. The O−O distances, marked by ↔, are calculated from the Li_2MnO_3 and $HCrO_2$ structures.

Samples from the Li_2MnO_3(A) series, which show only partial Li removal from the layers by NMR, show only unreacted Li_2MnO_3 and the sheared ($R\bar{3}m$) phase by XRD; thus, the NMR and the XRD show no evidence of solid-solution behavior. Partially protonated Li_2MnO_3 phases do not appear to be stable: once a Li layer is protonated, the exchange process (within this layer) proceeds to completion. This provides one explanation for why it is difficult to acid leach large Li_2MnO_3 particles, such as those synthesized at higher temperatures, because the activation energy required to shear the close-packed oxygen array to trigonal prismatic stacking should increase with increasing crystal size. The XRD data provided by Ooi and co-workers[6] do not provide clear evidence of the sheared structure (although we note that new reflections shifted to smaller values of 2θ from the position of the Li_2MnO_3 002 reflection are observed; Ooi and co-workers suggested that these are associated with a contraction of the O−O layers in Li_2MnO_3 due to hydrogen bonding). However, their electron microscopy data clearly show exfoliation of the large Li_2MnO_3 particles, with cleavage occurring between the layers to form large platelets with the same dimensions (in the *ab* planes) as the original Li_2MnO_3 particles. This is more pronounced for samples with $[H^+]$:$[Li^+]$ ratios of ≥0.25, as the extent of exfoliation increases with increasing $[H^+]$. We speculate that the same mechanism that causes shearing in our smaller Li_2MnO_3 particles also results in sufficient force to cleave the Li_2MnO_3 layers of larger particles, causing exfoliation. Ooi and co-workers have also suggested that stresses due to H^+/Li^+ exchange may be responsible for the cracking of these particles, although they do not describe a shearing mechanism.[6] The onset of the dissolution mechanism, only as the much larger Li_2MnO_3 particles start to crack, is consistent with this picture, dissolution occurring more readily at the cleaved surfaces.

3.2. Electrochemical Testing. Extended electrochemical tests were performed with Li_2MnO_3(B)_6 and Li_2MnO_3(B)_24 as electrode materials. Representative results are presented for Li_2MnO_3(B)_24, although the results for Li_2MnO_3(B)_6 are qualitatively similar. The electrochemical voltage profiles and capacity as a function of charging cycle are shown in Figure 9. The shape of the profile for the first few cycles, particularly those for discharge, suggests a single-phase insertion type of electrochemical reaction. The specific capacities for both materials are moderately high (≥150 mA·h/g). These capacities are consistent with the stoichiometries of the materials, and the reduction of Mn(IV) to Mn(III). For example, the electrochemical reaction for the sample

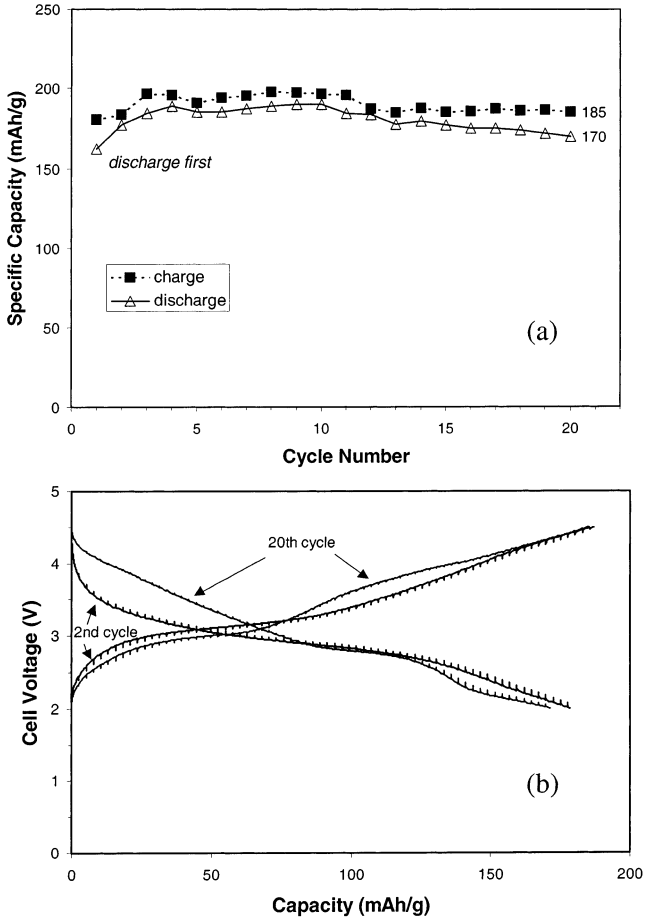

Figure 9. Galvanostatic cycling data of Li/Li_2MnO_3(B)_24 cells: (a) Specific capacity as a function of cycle number and (b) electrochemical profiles of the 2nd and 20th cycles. Current rate = 7.8 mA/g, potential range 4.5−2.0 V.

Li_2MnO_3(B)_24, which has a theoretical capacity of 292 mA·h/g (based on the Mn(IV) content) is

$$D_{0.22}[Li_{0.17}Mn_{0.83}]O_{1.86} + 0.83(Li^+ + e^-) \rightarrow D_{0.22}Li_{0.83}[Li_{0.17}Mn_{0.83}]O_{1.86} \quad (4)$$

The slightly higher first discharge capacity (162 mA·h/g) for the 24-h-leached sample, Li_2MnO_3(B)_24, compared with 151 mA·h/g for the 6-h-leached sample, Li_2MnO_3(B)_6, implies that there are more available sites for lithium to be filled electrochemically between the Mn/Li layers. This is in agreement with the proposed acid-leaching mechanism and the compositions for these two samples, additional acid treatment time resulting in greater removal of Li_2O in accordance with reaction 3. Similar capacities are seen for both samples in subsequent cycles.

Although the specific discharge capacities remain steady for 20 cycles, a comparison of the electrochemical profiles for the 2nd and 20th cycles indicate some differences in the electrochemical processes for the early and later cycles. The characteristic spinel features at 3 and 4−4.2 V are not clearly discerned, even following 20 cycles. However, the differences in the two profiles (particularly close to 3 and 4 V) indicate the onset of a transformation from the layered structure to a spinel-type structure, which has also been confirmed by cyclic

voltammetry;[24] however, this transformation is clearly suppressed in comparison to the electrochemical conversion of stoichiometric (layered) $LiMnO_2$ structure to spinel.[25] We suggest that the presence of both structurally bound protons and residual lithium in the manganese layers is an important feature that helps to slow the conversion of the layered structure to the spinel structure.

The second discharge capacity for both Li_2MnO_3(B)_6 and (B)_24 cathodes is slightly larger than the first discharge capacity. Furthermore, the capacity on the first charge is noticeably larger than the first discharge capacity. This additional capacity on charge cannot be associated with the manganese, the ^{6}Li NMR spectra providing no evidence for the presence of Mn(III) in the leached samples. Furthermore, it appears unlikely that this additional capacity is due to the correlated electrolyte breakdown and proton-for-lithium ion-exchange mechanism, which was shown to occur recently by Robertson and Bruce for Li_2MnO_3 during the first charge at approximately 4.4−4.6 V[10] because our materials are already ion-exchanged. We tentatively suggest that some of the increased capacity on the first charge is associated with the removal of some of the ion-exchanged protons, via reactions such as

$$H[Li_{0.33}Mn_{0.67}]O_2 \rightarrow H_{1-4\delta}[Li_{0.33}Mn_{0.67}]O_{2-2\delta} + 4e^- + 4\delta H^+ + O_2 \quad (5)$$

(written for simplicity for the ideal, ion-exchanged material). This reaction can be viewed as effectively removing structural water, but importantly it should create vacancies in the lithium layers, which can presumably accommodate lithium on discharging. On the basis of previous chemical lithiation studies with LiI,[4] the oxygen array can be expected to revert to close packing on subsequent discharging when the reaction will occur predominantly by the reinsertion of lithium ions, not protons. Differences in proton (deuteron) contents of the samples might be expected to alter the ease with which these shearing processes occur and affect the capacity retentions of these materials. Cyclic voltammetry and open-circuit-voltage measurements in combination with ^{6}Li and ^{2}H NMR experiments are currently in process to test these hypotheses and, in particular, to examine the effect of proton/lithium ion-exchange reactions[10] involving lithium ions or protons (created, for example, by reaction 5) in the electrolyte on the subsequent electrochemical performance of these materials and on the structural stability of the layered framework.

4. Conclusions

This work has demonstrated that lithium and deuterium NMR, in conjunction with X-ray diffraction, may be used to follow the acid leaching of Li_2MnO_3. XRD data confirm that acid leaching results in the shearing of the $[Li_{0.33}Mn_{0.67}]O_2$ layers, while ^{6}Li MAS NMR data of the same samples provide evidence that Li^+ is removed from the lithium layers, while lithium remains in the Li/Mn layers. The level of delithiation between the transition-metal layers (i.e., from the 4h and 2c sites in Li_2MnO_3) is proportional to the acid-leaching time. In contrast, a change only in the local environment, but not the content, of the lithium in the transition-metal layer is observed until most of the lithium in the lithium layers is extracted. A significant amount of lattice deuterons, present as −OD groups, are observed by deuterium NMR from the samples leached in D_2SO_4 (in D_2O), supporting the Li^+/H^+ ion-exchange mechanism suggested in related studies. Upon prolonged acid leaching, a decrease in both the lithium and deuterium content was observed, indicating that lithia (Li_2O) dissolution can also occur in conjunction with ion exchange. An electrochemical oxidative process is postulated to include the electrolysis of structural water in the acid-leached cathodes, which accounts for the higher charge capacity (to 4.5 V) and coulombic inefficiency in our extended electrochemical cycling studies of the samples.

Both the NMR approach and the structural and electrochemical properties of the acid-leached Li_2MnO_3 materials determined in this study may be important in understanding the electrochemical behavior of Li/Li_2MnO_3 cells reported in 1999 by Kalyani et al.[9] and more recently by Robertson and Bruce.[10] Ion-exchange reactions have also been suggested to occur in a range of other cathode materials, including lithium manganese spinels,[1,26] and ^{2}H MAS NMR is expected to find widespread use for investigating these and similar systems.

Acknowledgment. Financial support from the Office of Basic Energy Sciences and from the Office of Advanced Automotive Technologies of the U.S. Department of Energy and from the National Science Foundation (DMR9901308 and 0211353) is gratefully acknowledged.

CM0206385

(24) Kim, J.-S.; Johnson, C. S.; Thackeray, M. M. Unpublished results.

(25) Shao-Horn, Y.; Hackney, S. A.; Armstrong, A. R.; Bruce, P. G.; Gitzendanner, R.; Johnson, C. S.; Thackeray, M. M. *J. Electrochem. Soc.* **1999**, *146*, 2404.

(26) Ammundsen, B.; Aitchison, P. B.; Burns, G. R.; Jones, D. J.; Roziere, J. *Solid State Ionics* **1997**, *97*, 269.